

Gravitational lensing in modified Newtonian dynamics

Daniel J. Mortlock,^{1,2*} and Edwin L. Turner^{3*}

¹*Astrophysics Group, Cavendish Laboratory, Madingley Road, Cambridge CB3 0HE, U.K.*

²*Institute of Astronomy, Madingley Road, Cambridge CB3 0HA, U.K.*

³*Princeton University Observatory, Peyton Hall, Princeton, NJ 08544, U.S.A.*

Accepted. Received; in original form 2001 January 22

ABSTRACT

Modified Newtonian dynamics (MOND) is an alternative theory of gravity that aims to explain large-scale dynamics without recourse to any form of dark matter. However the theory is incomplete, lacking a relativistic counterpart, and so makes no definite predictions about gravitational lensing. The most obvious form that MONDian lensing might take is that photons experience twice the deflection of massive particles moving at the speed of light, as in general relativity (GR). In such a theory there is no general thin-lens approximation (although one can be made for spherically-symmetric deflectors), but the three-dimensional acceleration of photons is in the same direction as the relativistic acceleration would be. In regimes where the deflector can reasonably be approximated as a single point-mass (specifically low-optical depth microlensing and weak galaxy-galaxy lensing), this naive formulation is consistent with observations. Forthcoming galaxy-galaxy lensing data and the possibility of cosmological microlensing have the potential to distinguish unambiguously between GR and MOND. Some tests can also be performed with extended deflectors, for example by using surface brightness measurements of lens galaxies to model quasar lenses, although the breakdown of the thin-lens approximation allows an extra degree of freedom. Nonetheless, it seems unlikely that simple ellipsoidal galaxies can explain both constraints. Further, the low-density universe implied by MOND must be completely dominated by the cosmological constant (to fit microwave background observations), and such models are at odds with the low frequency of quasar lenses. These conflicts might be resolved by a fully consistent relativistic extension to MOND; the alternative is that MOND is not an accurate description of the universe.

Key words: gravitational lensing – relativity – gravitation – dark matter – acceleration of particles.

1 INTRODUCTION

Modified Newtonian dynamics (MOND; Milgrom 1983a) is an alternative theory of gravity in which either inertia or the effective gravitational force is changed in the limit of low accelerations (as opposed to large distances). Taken in its purest form, a MONDian universe would contain no dark matter, and be dominated by the low density of baryons generated in primordial nucleosynthesis (Sanders 1998; McGaugh 1999). MOND makes definite and generally successful predictions about the dynamics and properties of galaxies (Milgrom 1983b; Mateo 1998; McGaugh & de Blok 1998; Sanders 2000), groups (Milgrom 1998), clusters (Milgrom 1983c; Sanders 1994) and large-scale structure (Milgrom

1997). However MOND is not a complete physical theory – in particular it has no relativistic counterpart (Milgrom 1983a; Bekenstein & Milgrom 1984; Sanders 1997). Thus there are no concrete cosmological predictions, and it is not certain how photons couple to gravitational fields.

Despite the lack of any relativistic theory underpinning MOND, it is possible to constrain its properties by invoking the appropriate Newtonian limits and using basic symmetries. Felten (1984) and Sanders (1998) argued that the universe as a whole is in the Newtonian regime and so obeys the standard Friedmann equations,[†] and similarly that the

* E-mail: mortlock@ast.cam.ac.uk (DJM); elt@astro.princeton.edu (ELT)

[†] Thus the cosmology can be specified by the usual parameters: the normalised present day matter density, Ω_{m0} , the similarly normalised cosmological constant, $\Omega_{\Lambda0}$, and the Hubble constant, $H_0 = 100h \text{ km s}^{-1} \text{ Mpc}^{-1}$.

early universe is governed by general relativity (GR). Taking $H_0 = 70 \text{ km s}^{-1} \text{ Mpc}^{-1}$, and assuming a totally baryonic universe, the nucleosynthesis constraints of Tytler et al. (2000) imply that $\Omega_{\text{m}0} \simeq 0.01$. McGaugh (2000) showed that the CMB anisotropies measured by the MAXIMA-1 (Hannay et al. 2001) and BOOMERanG (de Bernardis et al. 2000) experiments are consistent with such a low-density cosmological model provided that the universe is spatially flat, i.e., $\Omega_{\Lambda 0} = 1 - \Omega_{\text{m}0} \simeq 0.99$. Despite these successes, there are a number of qualitative difficulties with a MONDian cosmology (e.g. Scott et al. 2001), although some are merely indicative of the great conceptual differences between MOND and more conventional physics.

There has been less focus on gravitational lensing within a MONDian framework, primarily as the deflection of light cannot be explained without recourse to a relativistic theory. Beckenstein & Sanders (1994) and Sanders (1997), in attempting to derive a relativistic extension of MOND, included gravitational lensing in their considerations, but a more empirical approach is adopted here. Mortlock & Turner (2001) used the galaxy-galaxy signal measured by Fischer et al. (2000) to constrain the deflection law of galaxies to be $A(R) \propto R^{0.1 \pm 0.1}$ over the range $10 \text{ kpc} \lesssim R \lesssim 1 \text{ Mpc}$. This is consistent with the deflection law obtained by assuming that, as in GR, photons experience twice the deflection of massive particles moving at the speed of light (Qin, Wu & Zhu 1995). Thus the asymptotic lensing effect of a MONDian point-mass matches that of an isothermal sphere, which in turn is consistent with most observations of lensing by galaxies (e.g. Brainerd, Blandford & Smail 1996; Kochanek 1996).

Encouraged by the qualitative agreement between data and observations, the lensing formalism of Qin et al. (1995) is explored in more detail here. In Section 2 a number of general results are derived and then applied to simple lens models. These are then compared to observations of galaxy-galaxy lensing (Section 3), microlensing (Section 4), multiply-imaged quasars (Section 5) and lensing by clusters (Section 6). The conclusions are summarised in Section 7.

2 MOND

MOND is most generally a modification of inertia (Milgrom 1983a), but, for gravitationally-dominated systems, can be more intuitively treated as an increase in the gravitational acceleration felt by test particles. The Newtonian acceleration due to a (static) mass distribution $\rho(\mathbf{r})$ is

$$\mathbf{a}_N(\mathbf{r}) = -G \iiint_{R^3} \rho(\mathbf{r}') \frac{\mathbf{r} - \mathbf{r}'}{|\mathbf{r} - \mathbf{r}'|^3} d^3 r', \quad (1)$$

where G is Newton's gravitational constant and \mathbf{r} is position[†]. The MONDian acceleration is related to this by (Milgrom 1983a)

$$\mathbf{a}(\mathbf{r}) f_M \left[\frac{a(\mathbf{r})}{a_0} \right] = \mathbf{a}_N(\mathbf{r}), \quad (2)$$

[†] Three-dimensional vectors are denoted by lower case (e.g. \mathbf{r}); two-dimensional vectors – projected onto the sky – are denoted by upper case (e.g. \mathbf{R}).

where a_0 is the critical acceleration, above which the dynamics is close to Newtonian. The exact form of $f_M(x)$ is not known, but $f_M(x) = 1$ if $x \gg 1$ and $f_M(x) = x$ if $x \ll 1$. No major MONDian results are sensitive to the form of this function in the regime $x \simeq 1$, and so

$$f_M(x) = \begin{cases} x, & \text{if } x < 1, \\ 1, & \text{if } x \geq 1 \end{cases} \quad (3)$$

is used here for mathematical simplicity. It is convenient to invert equation (2) so that the acceleration can be expressed as a function of known quantities. Defining a new function $f'_M(x)$ with the same asymptotic limits as $f_M(x)$, MOND may also be defined by

$$\mathbf{a}(\mathbf{r}) = f'_M{}^{-1/2} \left[\frac{a_N(\mathbf{r})}{a_0} \right] \mathbf{a}_N(\mathbf{r}). \quad (4)$$

For the particular choice of $f_M(x)$ given in equation (3), $f'_M(x) = f_M(x)$.

There are some difficulties in understanding equations (3) and (4) for complex systems (e.g. Milgrom 1983a; Scott et al. 2001), but their qualitative interpretation for a single particle is reasonably straightforward. For accelerations much greater than a_0 Newtonian dynamics remains valid, as $\mathbf{a}(\mathbf{r}) = \mathbf{a}_N(\mathbf{r})$. But if $a_N(\mathbf{r}) \ll a_0$ then $\mathbf{a}(\mathbf{r}) = [a_0 a_N(\mathbf{r})]^{1/2} \hat{\mathbf{a}}_N(\mathbf{r})$ and a test particle would feel an acceleration in the expected direction, but of a greater magnitude. The value of the critical acceleration has been determined from galaxy rotation curves as $a_0 = 1.2 \pm 0.1 \times 10^{-10} \text{ m s}^{-2}$ (Milgrom 1983b; Begeman, Broeils & Sanders 1991; McGaugh & de Blok 1998), and, modulo the uncertainty in the form of $f_M(x)$, MOND has no other free parameters. Equations (3) and (4) are sufficient to calculate the trajectory of a massive particle (Section 2.1), from which a natural formalism for the deflection of photons can be extrapolated (Sections 2.2 and 2.3).

2.1 Deflection of massive particles

Within the framework of MONDian (or Newtonian) dynamics it is possible to calculate the trajectory of an arbitrary particle. If, however, the particle is sufficiently light that it does not disturb the external mass distribution, and its speed is such that its path is nearly linear, its deflection can be approximated by integrating the acceleration along the unperturbed trajectory (i.e. a straight line). Without loss of generality, this path can be defined as being parallel to the z -axis of a Euclidean coordinate system, with $\mathbf{R} = (x, y)$ the two-dimensional impact parameter (relative to some reference point) in the plane of the sky. Thus the deflection angle, $\mathbf{A} = (A_x, A_y)$, of a particle moving with speed v in the z -direction is given by

$$\begin{aligned} A_i(\mathbf{R}) &\simeq \frac{v_i}{v} \\ &= \frac{1}{v} \int_{-\infty}^{\infty} a_i[\mathbf{r}(t)] dt \\ &= \int_{-\infty}^{\infty} f'_M{}^{-1/2} \left\{ \frac{a_N[\mathbf{r}(t)]}{a_0} \right\} a_{Ni}[\mathbf{r}(t)] dt, \end{aligned} \quad (5)$$

where $i \in \{x, y\}$, and $\mathbf{a}(\mathbf{r})$ is defined in equations (1) and (4). For a minimally-deflected particle, $\mathbf{r}(t) = [x, y, v(t-t_0)]$, where t_0 is an arbitrary reference time.

2.2 Deflection of photons

In the standard theory of gravitational lensing (e.g. Schneider, Ehlers & Falco 1992), the deflection of photons in weak, static gravitational fields can be calculated from GR, and is simply twice the deflection experienced by a massive particle moving at the speed of light, c . This has been confirmed observationally for light grazing the Sun (Dyson, Eddington & Davidson 1920; Robertson & Carter 1984) and this simple relationship must also be true of MONDian lensing in the Newtonian limit. There is no strong evidence that this relationship holds in the deep MONDian limit, but such a model is consistent with galaxy-galaxy lensing (Mortlock & Turner 2001), and this hypothesis is adopted henceforth. The deflection angle of photons can thus be read from equation (5) as

$$A_i(\mathbf{R}) = \frac{2}{c} \int_{-\infty}^{\infty} f_M'^{-1/2} \left\{ \frac{a_N[\mathbf{r}(t)]}{a_0} \right\} a_{Ni}[\mathbf{r}(t)] dt, \quad (6)$$

where again $i \in \{x, y\}$ and, for a photon, $\mathbf{r}(t) = [x, y, c(t-t_0)]$.

2.2.1 The thin-lens approximation

In the limit $a_0 \rightarrow 0$, the standard relativistic deflection formula can be reproduced by using equation (1) to obtain

$$A_{Ni}(\mathbf{R}) = \frac{2}{c} \int_{-\infty}^{\infty} a_{Ni}[\mathbf{r}(t)] dt. \quad (7)$$

In the limit of small deflection angles (relative to the line-of-sight extent of the lens) the thin-lens approximation (e.g. Schneider et al. 1992) can be invoked. Equation (7) can thus be reduced to

$$A_N(\mathbf{R}) = - \iint_{R^2} \frac{4G\Sigma(\mathbf{R}')}{c^2} \frac{\mathbf{R}' - \mathbf{R}}{|\mathbf{R}' - \mathbf{R}|^2} d^3R', \quad (8)$$

where the surface density of the lens is

$$\Sigma(\mathbf{R}) = \int_{-\infty}^{\infty} \rho(x, y, z) dz. \quad (9)$$

The application of the thin-lens approximation allows many lensing problems to be greatly simplified, and equation (8) is one of the main results of standard gravitational lensing theory.

As given in equation (6) the MONDian deflection angle cannot be simplified in general. In particular, there is no useful thin-lens approximation: equation (6) cannot be simplified in the same way that equation (7) can. More qualitative arguments imply that the same is likely to be true of any MONDian lensing theory (see Section 2.3.2). Further, constant mass-to-light ratio models of real gravitational lenses cannot reproduce the observed image configurations (e.g. AbdelSalam, Saha & Williams 1998; Section 5.1); this would almost certainly invalidate MOND if the thin-lens approximation were valid. The ambiguity in the line-of-sight mass distribution of an observed deflector is inconvenient (as is the extra integral required in the calculation of deflection

angles), but could be thought of as analogous to the a priori unconstrained dark matter distributions that dominate conventional gravitational lensing studies.

Despite the lack of a general thin-lens approximation, some simplifications of equation (6) are possible. In many cases the deflection angle can be decomposed into two MONDian segments (when the photon is far away from the lens) and a single Newtonian segment (the major deflection near the lens). If the deflector is sufficiently localised, the latter regime can be handled in the usual way, using the thin-lens formalism, and the MONDian contribution away from the lens may be approximated by the simple point-mass formula (Section 2.3.1), the deflector being ‘unresolved’ at such great distances.

2.2.2 The lens equation

Gravitational lensing can be thought of as a mapping between the source plane (an imaginary surface, perpendicular to the line-of-sight, on which a source is located) and the sky or image plane. The lens equation relates the angular position of a source, β , to the angular position(s) of its image(s), θ , and can be written as (cf. Schneider et al. 1992)

$$\beta = \theta + \alpha(\theta), \quad (10)$$

where

$$\alpha(\theta) = \frac{d_{ds}}{d_{os}} \mathbf{A}(d_{od}\theta). \quad (11)$$

In these definitions, d_{od} , d_{os} and d_{ds} are the angular diameter distances between observer and deflector, observer and source, and deflector and source, respectively. It is not entirely clear how they vary with redshift in a MONDian cosmology. Even if the universe obeys the Friedmann equation, as implied by the results of Sanders (1998), the separation of nearby photons can only be determined by a relativistic extension of MOND, although the standard distance measures should be reproduced in the limit of large angular separation (cf. Linder 1998). Where values of d_{od} , d_{os} and d_{ds} are required, they are calculated for the appropriate low-density Friedmann model using standard formulae (e.g. Carroll, Press & Turner 1992). This is probably consistent with the lensing theory described above, but is no more than a reasonable assumption.

The lens equation allows the calculation of image positions, magnifications and distortions. The magnification of a single image is (Schneider et al. 1992)

$$\mu(\theta) = \left| \frac{d^2\beta}{d\theta^2} \right|^{-1}, \quad (12)$$

and the total magnification of a source is then

$$\mu_{\text{tot}}(\beta) = \sum_{i=1}^{N_i} \mu[\theta_i(\beta)], \quad (13)$$

where the sum is over the N_i images formed, and $\theta_i(\beta)$ is the position of the i th image.

2.2.3 Spherical symmetry

If the deflector is spherically symmetric, then $\rho(\mathbf{r}) = \rho(r)$ and equation (6) can be written as

$$\mathbf{A}(\mathbf{R}) = -\frac{2G}{c^2}\mathbf{R} \quad (14)$$

$$\times \int_{-\infty}^{\infty} f'_M{}^{-1/2} \left[\frac{GM(<\sqrt{R^2+z^2})}{(R^2+z^2)a_0} \right] \frac{M(<\sqrt{R^2+z^2})}{(R^2+z^2)^{3/2}} dz,$$

where

$$M(<r) = \int_0^r 4\pi r'^2 \rho(r') dr'. \quad (15)$$

It is possible to write down an analogue of the usual lens equation by expressing $M(<r)$ in terms of the projected surface density. Using equation (15) and expressing $\rho(r)$ in terms of an Abel integral (e.g. Binney & Tremaine 1987),

$$\begin{aligned} M(<r) &= \int_0^r 4\pi r'^2 \int_{r'}^{\infty} -\frac{1}{\pi} \frac{d\Sigma}{dR} \frac{1}{\sqrt{R^2-r'^2}} dR dr', \\ &= 2 \int_r^{\infty} \left[\frac{r}{R} \sqrt{1 - \frac{r^2}{R^2}} - \arcsin\left(\frac{r}{R}\right) \right] R^2 \frac{d\Sigma}{dR} dR \\ &\quad - \pi \int_0^r R^2 \frac{d\Sigma}{dR} dR, \end{aligned} \quad (16)$$

where the order of integration is reversed, making the inner integral trivial (cf. Kovner 1987). This formula is not particularly useful for unbounded mass distributions like the isothermal sphere (Section 2.3.3), as its convergence properties are poor. However in the case of MOND galactic mass distributions fall off as fast as their luminosity density – exponentially, in general – and so equation (16) is well behaved, as well as relating the observed surface brightness of a deflector directly to its lensing properties.

The combination of equations (14) and (16) are suggestive of an alternative formalism for spherical lenses. MONDian lensing can be cast in terms of the conventional formalism of Schneider et al. (1992) if an ‘effective’ surface density is defined. Specifying it by either $\rho_N(r)$ or $\Sigma_N(R)$ (as it is only relevant in the symmetric case), it is the density profile that would, under the assumption of Newtonian mechanics, produce both the same rotation curve and the same deflection law as the model profile produces in MOND. Given that a point-mass has an asymptotically constant rotation speed of $v_c = (GMa_0)^{1/4}$ in MOND (Milgrom 1983b), the addition of an isothermal component is suggested, and defining

$$\rho_N(r) = \rho(r) + \frac{M^{1/2}a_0^{1/2}}{4\pi G^{1/2}r^2} \quad (17)$$

is a reasonable approximation to many MONDian deflectors of true mass M . The same rotation curves and deflection laws would result from defining $f_M(x) = 1 + [1 + (1 + 4x)^{1/2}]/(2x)$.

In the limit of $f'_M(x) \rightarrow 1$ and $a_0 \rightarrow 0$, equation (14) reduces to the conventional result that (e.g. Schneider et al. 1992)

$$\mathbf{A}_N(\mathbf{R}) = -\frac{4G}{c^2} \frac{M(<R)}{R^2} \mathbf{R}, \quad (18)$$

where

$$M(<R) = \int_0^R 2\pi R' \Sigma(R') dR'. \quad (19)$$

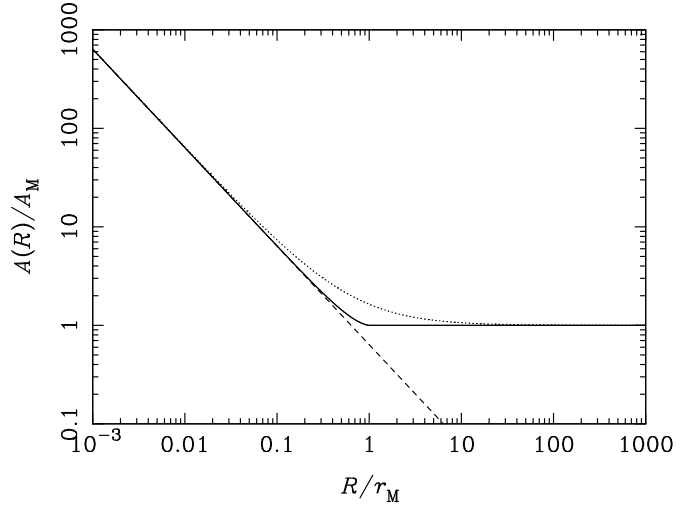


Figure 1. The deflection law of a point-mass in MOND (solid line) and GR (dashed line). The dotted line shows the approximation to the MONDian result obtained by calculating the Newtonian deflection caused by an isothermal sphere superimposed on a point-mass (see Section 2.2.3).

2.3 Lens models

Having developed a plausible formalism for gravitational lensing within the framework of MOND, more specific results can be derived for some simple mass distributions.

2.3.1 Point-mass

For a point lens of mass M , $\rho(\mathbf{R}) = M\delta^3(\mathbf{R})$ and $M(<R) = M$. Using the piecewise definition of $f'_M(x)$, equation (14) splits up into several trivial integrals, and the deflection law for a point-mass is given by

$$A(R) = \begin{cases} -\frac{4GM}{c^2 R} \sqrt{1 - \frac{R^2}{r_M^2}} \\ -A_M \left[1 - \frac{2}{\pi} \arctan\left(\sqrt{\frac{r_M^2}{R^2} - 1}\right) \right], & \text{if } R \leq r_M, \\ -A_M & \text{if } R > r_M, \end{cases} \quad (20)$$

where $r_M = (GM/a_0)^{1/2}$ is the distance from a point-mass at which the physics changes from the Newtonian to the MONDian regime and $A_M = 2\pi(GMa_0)^{1/2}/c^2$ is the asymptotic MONDian deflection angle. This is compared to the standard point-mass deflection angle (as inferred from the Schwarzschild metric) in Fig. 1. For large impact parameters ($R \gtrsim r_M$) the photon experiences an acceleration of less than a_0 , and so the deflection angle is independent of impact parameter, in much the same way that the rotation speed would be. For $R \lesssim r_M$, the light path is in the MONDian regime for the most part (the second term in the above formula), but the deflection is dominated by the Newtonian force close to the lens (the first term, which approaches the Schwarzschild bending angle for small R).

The next step in analysing the point-mass lens is to convert equation (20) into angular units, in order to write down the lens equation. The Schwarzschild lens is completely characterised by its Einstein angle,

$$\theta_E = \sqrt{\frac{4GM}{c^2} \frac{d_{ds}}{d_{od}d_{os}}}, \quad (21)$$

but two other angular scales are useful here:

$$\theta_M = \frac{r_M}{d_{od}} = \sqrt{\frac{GM}{d_{od}^2 a_0}}, \quad (22)$$

beyond which the deflection angle becomes constant; and

$$\alpha_M = \frac{2\pi\sqrt{GMa_0}}{c^2} \frac{d_{ds}}{d_{os}} = \frac{\pi}{2} \frac{\theta_E^2}{\theta_M}, \quad (23)$$

the value of the deflection angle in this regime. Combining the above definitions with equation (11), equation (20) reduces to

$$\alpha(\theta) = \quad (24)$$

$$\begin{cases} -\frac{\theta_E^2}{\theta} \sqrt{1 - \frac{\theta^2}{\theta_M^2}} \\ -\alpha_M \left[1 - \frac{2}{\pi} \arctan \left(\sqrt{\frac{\theta_M^2}{\theta^2} - 1} \right) \right], & \text{if } \theta \leq \theta_M, \\ -\alpha_M, & \text{if } \theta > \theta_M, \end{cases}$$

with $\alpha(\theta_M) \simeq -\alpha_M$. From equation (12) the magnification of a single image is then

$$\mu(\theta) = \quad (25)$$

$$\begin{cases} \theta^4 \theta_M^2 / \left| \left(\theta^2 \theta_M + \theta_E^2 \sqrt{\theta_M^2 - \theta^2} \right) \left\{ \theta^2 \theta_M - \theta_E^2 \sqrt{\theta_M^2 - \theta^2} \right. \right. \right. \\ \left. \left. \left. - \alpha_M \theta \theta_M \left[1 - \frac{2}{\pi} \arctan \left(\sqrt{\frac{\theta_M^2}{\theta^2} - 1} \right) \right] \right\} \right|, & \text{if } \theta \leq \theta_M, \\ \theta / (\theta - \alpha_M), & \text{if } \theta > \theta_M, \end{cases}$$

whereas for a Newtonian point-mass it is simply $\mu_N(\theta) = |\theta^4 / (\theta^4 - \theta_E^4)|$.

Inverting the lens equation [equation (10)] and using the magnification formulæ given in equation (13) and (25) allows $\mu_{\text{tot}}(\beta)$ to be calculated. This is shown in Fig. 2, with the x -axis normalised to match the Newtonian Einstein radius. In all cases $\mu_{\text{tot}}(\beta)$ matches the relativistic form for $\beta \lesssim \theta_M$; beyond that MOND always results in a greater magnification. The shapes of these curves are determined by the mass-independent ratio of the Einstein angle to the characteristic MONDian angular scale. From equations (21) and (22) this ratio is given by

$$\frac{\theta_E}{\theta_M} = \sqrt{\frac{4a_0}{c^2} \frac{d_{od}d_{ds}}{d_{os}}} \lesssim 0.006 \left(\frac{d_{os}}{1 \text{ Mpc}} \right)^{1/2} \simeq 0.35 z_s^{1/2}, \quad (26)$$

where the upper limit is calculated by assuming that $d_{od} \simeq d_{ds} \simeq d_{os}/2$, and the last expression is valid only in the local universe, where $d_{os} = cz_s/H_0$. This ratio is shown in Fig. 3: its increase with z_s is quite apparent, and it is also important that it does not vary greatly with z_d unless either d_{od} or d_{ds} is close to zero. Within the Galaxy MONDian lensing effects should be minimal, with $\theta_E/\theta_M \lesssim 0.001$, but they could become very important on cosmological scales, a point which is explored in more detail in Section 4.

2.3.2 Thin rod

In the standard theory of gravitational lensing, the deflection properties of most isolated mass distributions depend only

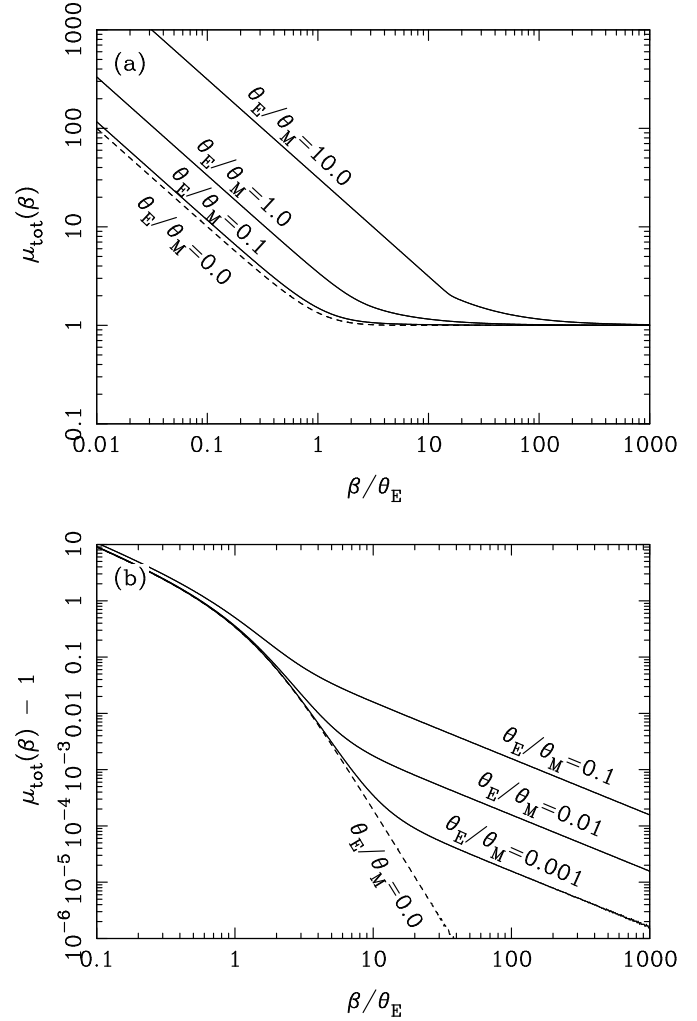


Figure 2. The total magnification of a source as a function of its angular separation, β , from the optical axis of a MONDian point-mass deflector. More extreme effects are emphasised in (a) and weaker effects shown in (b). The solid curves show increasing values of θ_E/θ_M , as labelled; the dashed curves show the Newtonian result (which could also be obtained by taking $\theta_E/\theta_M = 0$). Note that θ_E is the Einstein angle of the Newtonian point-mass; the x -axis could also be normalised by the actual Einstein angle of the lens, which increases as θ_M decreases. This approach is taken in Fig. 6.

on their projected surface density. As argued in Section 2.2 the thin-lens approximation is unlikely to hold in MOND, and this can be illustrated by considering the lensing effect of a thin rod oriented along the line-of-sight. Its density is given by

$$\rho(\mathbf{r}) = \begin{cases} 0, & \text{if } z < -l/2, \\ M/l \delta^2(\mathbf{R}), & \text{if } -l/2 \leq z \leq l/2 \\ 0, & \text{if } z > l/2, \end{cases} \quad (27)$$

where M is the rod's mass and l its length. Inserting this definition into equation (6) and evaluating the required integrals gives the Newtonian acceleration as

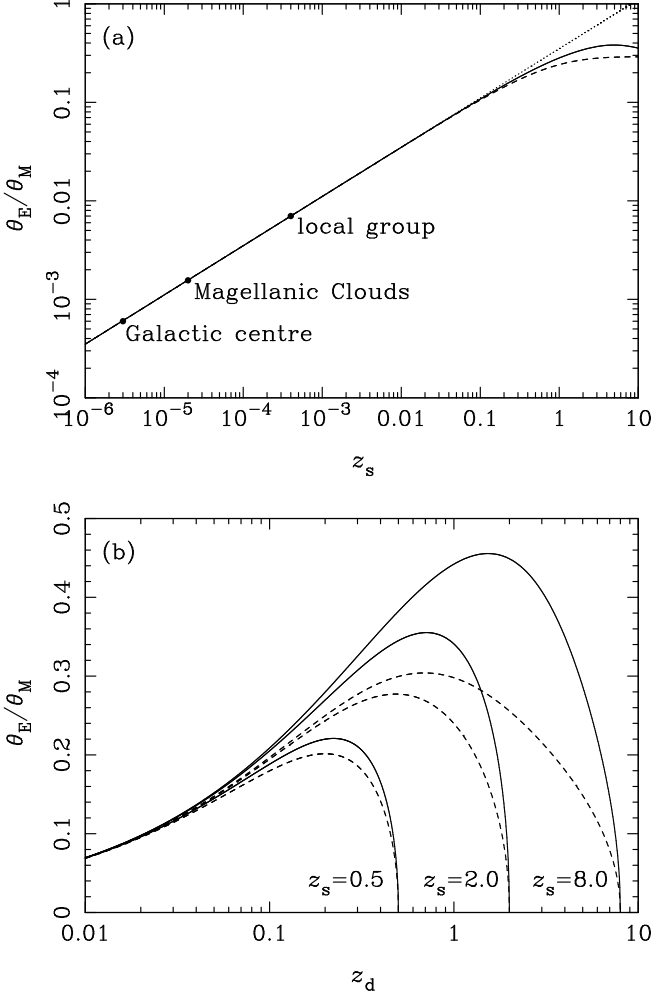


Figure 3. The ratio of the Einstein angle of a point-mass, θ_E , to its characteristic MONDian angular scale, θ_M , as a function of source redshift, z_s (a) and deflector redshift, z_d (b). In (a) the deflector is assumed to be halfway between observer and source, and in (b) results are shown for several source redshifts, as indicated. Two cosmological models are shown: $\Omega_{m0} = 0.01$ and $\Omega_{L0} = 0.99$ (solid lines); and $\Omega_{m0} = 0.01$ and $\Omega_{L0} = 0.0$ (dashed lines); the dotted line in (a) is given by $\theta_E/\theta_M = 0.35z_s^{1/2}$, which is a good approximation in the local universe. Scales corresponding to the Galactic centre, the Magellanic Clouds, and the local group are marked, with the ‘effective redshift’ given by $z_s = H_0/c d_{os}$.

$$\begin{aligned}
 a_{N_x} &= -\frac{GM}{l} \frac{x}{R^2} \left[\frac{z+l/2}{\sqrt{R^2 + (z+l/2)^2}} - \frac{z-l/2}{\sqrt{R^2 + (z-l/2)^2}} \right], \\
 a_{N_y} &= -\frac{GM}{l} \frac{y}{R^2} \left[\frac{z+l/2}{\sqrt{R^2 + (z+l/2)^2}} - \frac{z-l/2}{\sqrt{R^2 + (z-l/2)^2}} \right], \\
 a_{N_z} &= -\frac{GM}{l} \left[\frac{1}{\sqrt{R^2 + (z-l/2)^2}} - \frac{1}{\sqrt{R^2 + (z+l/2)^2}} \right],
 \end{aligned}
 \tag{28}$$

where, as before, $R^2 = x^2 + y^2$. The MONDian acceleration can be calculated directly from this using equation (2), but the results are cumbersome and so not presented in full.

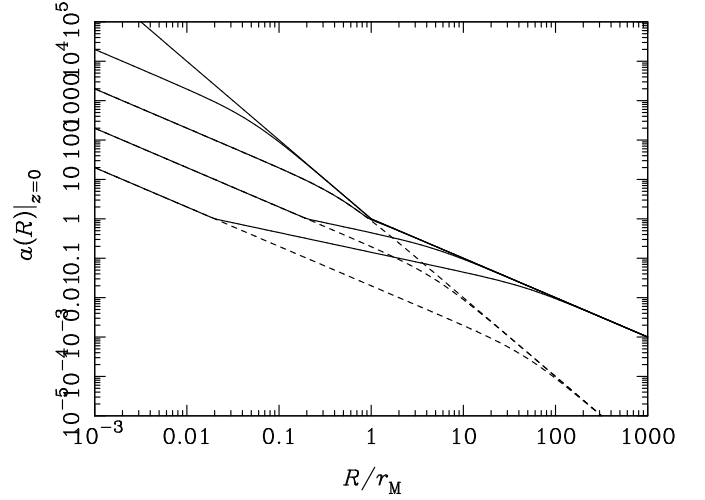


Figure 4. The equatorial acceleration produced by a thin rod (oriented along the z -axis) in MOND (solid lines) and GR (dashed lines). Here r_M is the radius at which the acceleration becomes MONDian for the corresponding point-mass. Curves are shown for several lengths: 0; $0.1r_M$; r_M ; $10r_M$; and $100r_M$, with the acceleration decreasing (at least for $r < r_M$) as length increases.

Some idea of the lensing properties of such an object can be gained by looking at the acceleration in the x - y plane. Applying the definitions given in Section 2 yields an ‘equatorial’ MONDian acceleration (directed towards the origin) of magnitude

$$a(R)|_{z=0} = \begin{cases} \frac{GM}{R} [R^2 + (l/2)^2]^{-1/2}, & \text{if } R \leq R_M, \\ \sqrt{\frac{GM a_0}{R}} [R^2 + (l/2)^2]^{-1/4}, & \text{if } R > R_M, \end{cases}
 \tag{29}$$

where

$$R_M = \frac{l}{2} \frac{1}{\sqrt{2}} \left[\sqrt{1 + 4 \left(\frac{r_M}{l/2} \right)^4} - 1 \right]^{1/2}
 \tag{30}$$

is the equatorial radius at which the acceleration equals a_0 , and r_M is the MONDian radius of the equivalent point-mass. A family of these curves is shown in Fig. 4, with the Newtonian accelerations also included for comparison. Close to the rod $a(R) \propto R^{-1}$, the standard Newtonian result, and for very large impact parameters $a(R) \propto R^{-1}$, the rod acting like a MONDian point-mass. In most cases there is an intermediate region in which the acceleration is sufficiently small to feel a MONDian boost but the rod’s finite length is also important. The combination of these two effects results in a $a(R) \propto R^{-1/2}$ dependence, and any particle passing through this region would feel an unusually large gravitational pull.

It is also revealing to consider how the acceleration varies along the z -axis. Taking $x = y = 0$ in equation (28) and again applying MONDian dynamics (outside the length of the rod) yields

$$a(0, 0, z) =
 \tag{31}$$

$$\begin{cases} -\frac{GM}{l} \left(\frac{1}{|z|-l/2} - \frac{1}{|z|+l/2} \right) \hat{z}, & \text{if } l/2 < |z| \leq z_M, \\ -\sqrt{\frac{GMa_0}{l}} \left(\frac{1}{|z|-l/2} - \frac{1}{|z|+l/2} \right)^{1/2} \hat{z}, & \text{if } |z| > z_M, \end{cases}$$

where

$$z_M = \frac{l}{2} \sqrt{1 + \left(\frac{r_M}{l/2} \right)^2}. \quad (32)$$

Note that if $l \gg r_M$ the acceleration becomes MONDian for $|z| \gtrsim l/2$, i.e. anywhere outside the rod.

The integrals required to obtain the deflection angle must be calculated numerically, and the results are shown in Fig. 5. If $R \ll R_M$ then the deflection is essentially Newtonian [i.e. $A(R) \rightarrow 4GM/(c^2 R)$] as the deflection is dominated by the portion of the photon path alongside the rod. The opposite extreme is if $R \gg l$, in which case the rod acts like a point-mass, being ‘unresolved’ by the photon. Thus $A(R) \rightarrow 2\pi(GMa_0)^{1/2}/c^2 = A_M$ in this regime, provided that the rod is of finite length[§]. A corollary of these two arguments is that the thin-lens approximation is valid in MOND if the line-of-sight extension of the deflector is less than r_M , as, for all impact parameters, the deflection is either Newtonian or effectively point-like. However if $l \gtrsim r_M$ then $A(R) \propto R^{-1/2}$ for $R_M \lesssim R \lesssim l$. In this case the photon’s deflection is dominated by a segment of length $\sim l$ during which it feels a nearly perpendicular acceleration of $a \simeq [2GMa_0/(Rl)]^{1/2}$. Thus the deflection angle is $A(R) \simeq 2/c^2 (2GMa_0 l/R)^{1/2}$ in this region, and is proportional to the line-of-sight extent of the deflector.

The differences between the curves in Fig. 5 give some idea of the validity of the thin-lens approximation for an isolated deflector. For example, a typical elliptical galaxy with its major axis along the line-of-sight would have an effective l of ~ 10 kpc or more (Section 3) and $r_M \simeq 2$ kpc, which would imply that the thin-lens approximation is probably reasonable in this situation.

2.3.3 Isothermal sphere

The isothermal sphere (e.g. Binney & Tremaine 1987) is a useful and simple galaxy model within the dark matter paradigm as it explains the flat rotation curves of spirals, the dynamics of ellipticals, and the lensing properties of both. Parameterised by its (unobservable) velocity dispersion, σ , and its core radius, r_c , its density is given by (e.g. Hinshaw & Krauss 1987)

$$\rho_N(r) = \frac{\sigma^2}{2\pi G} \frac{1}{R^2 + r_c^2}. \quad (33)$$

Given the choice of $f_M(x)$ described in Section 2, the gravitational properties of this model can be almost exactly replicated in MOND by the density profile

$$\rho(r) = \begin{cases} \frac{\sigma^2}{2\pi G} \frac{1}{R^2 + r_c^2}, & \text{if } r \leq r_M, \\ 0, & \text{if } r > r_M, \end{cases} \quad (34)$$

[§] An infinitely long rod has an infinite deflection angle, irrespective of impact parameter.

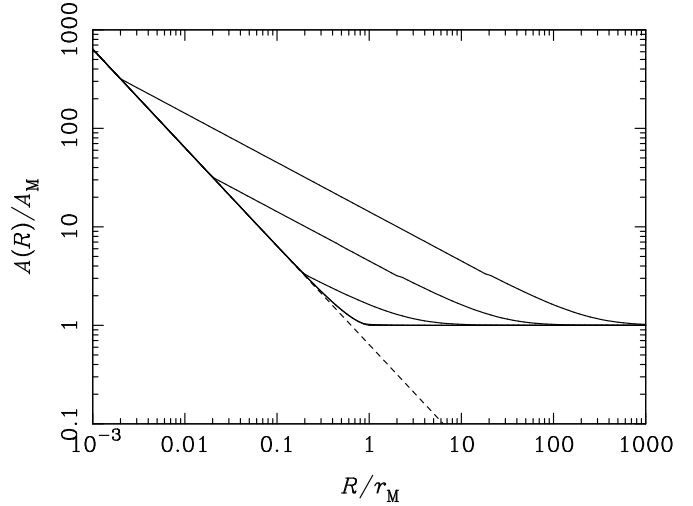


Figure 5. The deflection law of a thin rod oriented along the line-of-sight in MOND (solid lines) and GR (dashed line). Here r_M is the radius at which the acceleration becomes MONDian for the corresponding point-mass, and A_M is the asymptotic constant deflection angle. Curves are shown for several lengths: 0; r_M (almost indistinguishable from $l = 0$); $10r_M$; $100r_M$; and $1000r_M$, with the deflection angle increasing with length.

assuming $r_c \ll r_M$, which is certainly the case for real galaxies. The image positions and magnifications produced by such a mass distribution could be obtained from the MONDian formalism (Section 2), but there is no need to perform these calculations explicitly, as its lensing properties match those of the conventional isothermal sphere, which has been studied in great detail (e.g. Hinshaw & Krauss 1987; Kochanek 1996; Mortlock & Webster 2000). In particular, standard calculations of lens statistics remain valid, a point explored in more detail in Section 5.2.

3 GALAXY-GALAXY LENSING

Background galaxies are observed to be tangentially aligned around foreground galaxies due to the latter population’s gravitational lensing effect. Termed galaxy-galaxy lensing, this technique has – under the assumption of GR – confirmed the existence of extended isothermal haloes around all types of galaxies (e.g. Brainerd et al. 1996; Fischer et al. 2000). However it is potentially an even more powerful probe of alternative gravity theories as the shear signal extends far enough beyond the visible extent of the deflectors that they can be treated as point-masses. The radial dependence of the shear signal is consistent with the MONDian lensing formalism described in Section 2 (Mortlock & Turner 2001), and the forthcoming Sloan Digital Sky Survey (SDSS; York et al. 2000) data should allow measurements out to physical separations of ~ 1 Mpc. Beyond this the influence of secondary deflectors will start to dilute the signal, but, if MOND returns to a Newtonian regime at ultra-low accelerations ($\sim 10^{-12} \text{ m s}^{-2}$), the resultant cut-off might be detectable.

The full SDSS data-set will also facilitate a number of more general tests which should be able to discriminate between dark matter and alternative gravity theories unambiguously. These are discussed in detail by Mortlock &

Turner (2001), and so only summarised here. One implication of MOND is that the shear signal around any subset of the foreground population should have the same functional form, within the errors; any departure from this would represent strong evidence against such a model. A more powerful idea is to search for any deviation from azimuthal symmetry in the lensing signal (cf. Natarajan & Refregier 2000). A positive detection would be difficult to reconcile with MOND (or any alternative gravity theory with basic symmetry properties); a symmetric signal, on the other hand, would be in conflict with dark matter-based halo formation models (e.g. Navarro, Frenk & White 1995, 1996).

4 MICROLENSING

Microensing is the term used to describe the lensing action of (collections of) individual stars, and has been observed over a wide range of scales, from within the Galactic halo to redshifts of order unity. As the name suggests, the resultant image separations are much smaller than present day telescopes can resolve, and its only observable consequence is the change in magnification of a source caused by the relative motion of the deflector(s) across the line-of-sight.

Given that the additive nature of MONDian lensing is unknown, this discussion of microlensing will be limited to isolated deflectors, primarily single stars. For a point-source of unlensed magnitude m_0 , the resultant light-curve takes the form (cf. Paczyński 1986)

$$m(t) = m_0 - 2.5 \log \left\{ \mu_{\text{tot}} \left[\beta_0 \sqrt{\left(\frac{\beta_{\text{min}}}{\beta_0} \right)^2 + \left(\frac{t - t_{\text{min}}}{t_0} \right)^2} \right] \right\}, \quad (35)$$

where $\mu_{\text{tot}}(\beta)$ is given in Section 2.3.1, $\beta_{\text{min}}/\beta_0$ characterises the greatest alignment of deflector and source, t_0 is the time required for the alignment to change by angle β_0 , and t_{min} is the time at which the greatest alignment occurs. The choice of β_0 is somewhat arbitrary, but it is usual to define $\beta_0 = \theta_E$, which implies that $\mu_{\text{tot}}(\beta_0) = 1.34$ in GR. This last relation is taken to define β_0 here, which then implies that $\beta_0 \geq \theta_E$ in general, with equality in the limiting case of $\theta_M \rightarrow \infty$.

Several MONDian microlensing light-curves are shown in Fig. 6. The distinction between MOND and GR is clear if $\theta_E/\theta_M \gtrsim 1$; otherwise the only difference between the light-curves is in the $m(t) \simeq m_0$ wings. The ratio θ_E/θ_M depends mainly on the observer-source distance (Section 2.3.1), and only approaches unity if $z_s \gtrsim 1$ (Fig. 3). In physical terms, microlensing is useful as a probe of gravitational theories if the magnification is significant along geodesics passing beyond the Newtonian region of the deflector. This is not the case for microlensing within the local group (Section 4.1), but is true (in a MONDian universe) on cosmological scales (Section 4.2).

4.1 Microlensing within the local group

The vast majority of discrete microlensing events observed to date have been detected during the various monitoring programs (e.g. Afonso et al. 1999; Alcock et al. 2000; see Paczyński 1996 for a review) directed at either the Galactic

centre or the Magellanic Clouds, for which $d_{\text{os}} \lesssim 60$ kpc. Pixel lensing studies of M 31 (e.g. Gyuk & Crotts 2000; Cheongho & Gould 1996) have extended the distance scale to ~ 1 Mpc, but this is still too nearby to be very sensitive to MONDian effects. Equation (26) and Fig. 3 imply that $\theta_E/\theta_M \lesssim 0.005$ for all microlensing events within the local group. Basic lensing theory (e.g. Schneider et al. 1992) is then sufficient to show that only sources magnified by less than one per cent would be subject to any additional MONDian boost. To detect these changes, relative photometry accurate to ~ 0.001 mag would be required, and so there is little chance of constraining alternative gravity theories from the data currently available on single light-curves.

Future observations of local group microlensing events might include very accurate photometric monitoring for long periods after the magnification peak, but the distinction between MONDian and relativistic curves would only become apparent on scales where other deflectors along the line-of-sight start to have an effect. One promising avenue of investigation is to ‘stack’ the light-curves of simple microlensing events (i.e. in which both the deflector and source are point-like); this is discussed in a more general context in Mortlock & Turner (2001). Such an approach would not only allow a distinction to be made between GR and MOND, but it would also facilitate a measurement of $f_M(x)$ (defined in Section 2).

4.2 Cosmological microlensing

For sources at redshifts of $\gtrsim 1$ the Einstein radius and MOND radius of a point-mass deflector become comparable [equation (26) and Fig. 3]. The resultant microlensing light-curves are then quite different, as illustrated in Fig. 6, and there is the possibility of a clean and simple test to distinguish between GR, MOND, and other gravitational theories (Mortlock & Turner 2001).

In order to test these predictions, accurate photometry of cosmological microlensing by an isolated deflector is required. Such data could be forthcoming from the quasar monitoring programs being undertaken by Walker (1999) and Tadros, Warren & Hewett (2001). The idea of both experiments is to observe quasars seen through galactic or cluster haloes in the hope of a positive detection of compact dark matter. If MOND is correct then many of these targets should show no signs of microlensing, as they lie along empty (i.e. dark) lines-of-sight, which should be devoid of any potential deflectors in this model (e.g. Walker 1994; Mortlock & Turner 2001). It is thus quite likely that serendipitous observations of microlensing may provide the desired data, and indeed the spurious peak in the light-curve of gamma ray burst (GRB) 000301C (Sagar et al. 2000, and references therein) may be the result of microlensing (Garnavich, Loeb & Stanek 2000). Unfortunately the uncertainties in the photometry and lack of knowledge of the source geometry prevent any discrimination between MOND and GR (Mortlock & Turner 2001). Nonetheless, more events should be forthcoming, and cosmological microlensing has the potential to be a very clean method by which to measure the deflection law of a point-mass.

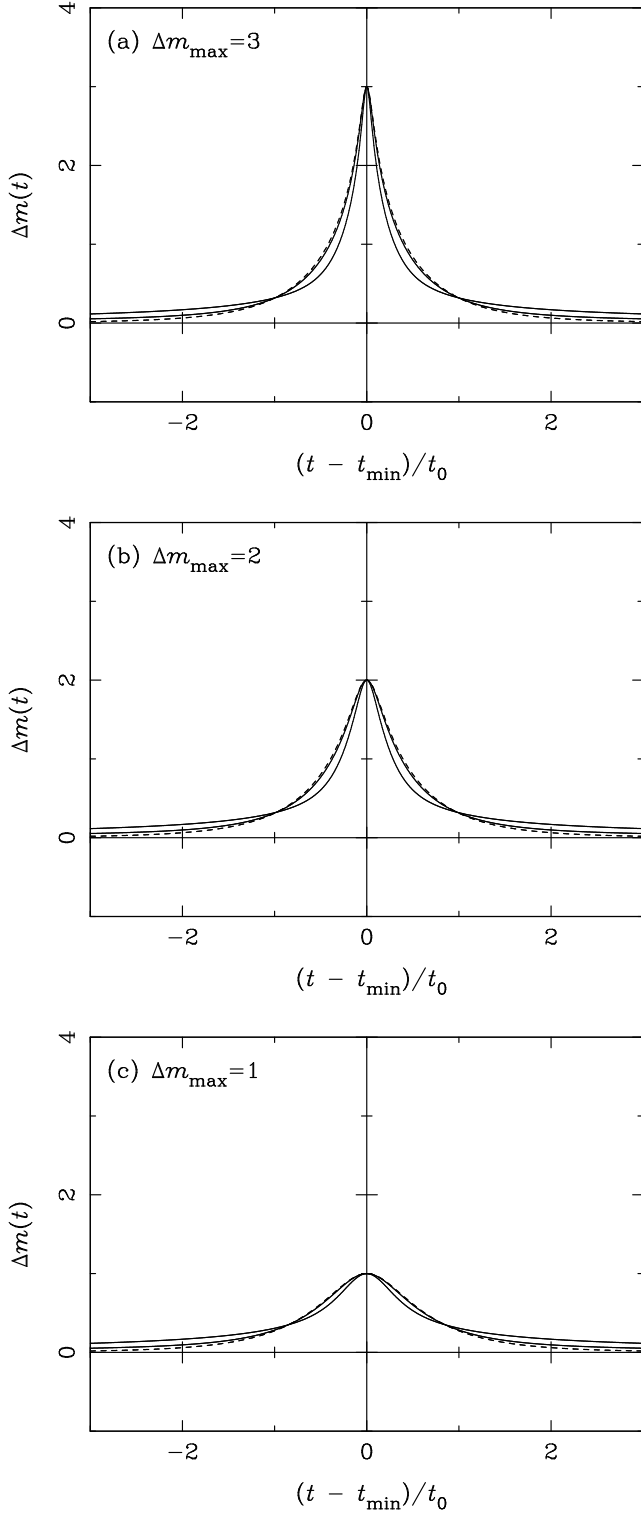


Figure 6. Microlensing light-curves, $\Delta m(t) = m_0 - m(t)$, calculated assuming MOND (solid lines) and GR (dashed lines). Each panel shows a different peak magnification (as labelled), and in each case the Einstein radius (i.e. the mass of the deflector) and minimum impact parameter are chosen to best fit the Newtonian result. For each value of Δm_{\max} light-curves are for $\theta_E/\theta_M = 0.0$ (i.e. GR), $\theta_E/\theta_M = 0.1$ and $\theta_E/\theta_M = 1.0$.

5 QUASAR LENSING

Since the identification of the first gravitationally-lensed object – Q 0957+561 (Walsh, Carswell & Weymann 1979) – there have been more than fifty quasar lenses discovered. The image configurations have been used to map the dark matter in the lens galaxies (e.g. Chen, Kochanek & Hewitt 1995; Chae, Turnshek & Khersonsky 1998; Keeton, Kochanek & Falco 1998), and the fraction of quasars which are lensed places strong limits on the cosmological model (e.g. Kochanek 1996). In the context of a MONDian universe, individual lenses can be used to constrain the deflection law of an extended mass distribution (Section 5.1) and the lens statistics are similarly revealing in a global context (Section 5.2).

5.1 Lens modeling

If there is no dark matter then it must be possible to model any quasar lens with a mass distribution that, when integrated along the line-of-sight, also matches the observed surface brightness of the deflector. Other mass concentrations along the line-of-sight may also have some influence (e.g. Keeton, Kochanek & Seljak 1997), but this is potentially a very powerful test of MOND.

The fact that the three-dimensional mass distribution is required to perform such a test suggests elliptical galaxies as deflectors, and several cases of lensing by (apparently) isolated ellipticals have already been discovered: e.g. MG 1654+1346 (Langston et al. 1989); MG 1549+3047 (Lehár et al. 1993); HST 1253–2914 (Ratnatunga et al. 1995); and HST 14176+5226 (Ratnatunga et al. 1995). Assuming that the deflector is a triaxial ellipsoid, the constraints implied by the observed surface brightness distribution leave only one free parameter, which is essentially the unknown extension of the galaxy along the line-of-sight. This is sufficiently restrictive that a successful fit would probably represent positive evidence in favour of MOND. However preliminary investigations suggest that such modeling cannot always produce a good fit to both photometric and lensing data, which would pose serious problems for the MONDian lensing theory put forward in Section 2.

5.2 Lens statistics

The fraction of high-redshift sources that are multiply-imaged increases rapidly with the cosmological constant as the co-moving volume element in an Ω_{Λ_0} -dominated universe is so high (Turner 1990). Kochanek (1996) used a selection of optical data and sophisticated modeling to show that the low observed number of lenses implies $\Omega_{\Lambda_0} < 0.65$ (with 95 per cent confidence), a limit which is only marginally consistent with the conventional dark matter-dominated universes preferred by CMB data and high-redshift supernova observations (e.g. Efstathiou et al. 1999). As a MONDian universe is likely to obey the Friedmann equations (Sanders 1998), these lensing results are completely at odds with the $\Omega_{m_0} \simeq 0.01$, $\Omega_{\Lambda_0} \simeq 0.99$ model described in Section 1. With the matter density limited by nucleosynthesis, the universe must be dominated by the vacuum energy density in order to satisfy the CMB power spectrum (McGaugh 2000). Thus it seems that no single cosmological model can explain lens

statistics, supernova data and CMB anisotropies within the framework of MOND.

One possible flaw in the above arguments is the assumed form of the angular diameter distance, which is not known with any certainty in MOND. The lens statistics are mildly sensitive to the distance formula used (Ehlers & Schneider 1986); the main aim of the supernova observations is to measure the luminosity distance; and the angular scale of the first peak in the CMB power spectrum only implies a flat universe if the angular diameter distance (on degree scales) obeys the standard formulae (e.g. Carroll et al. 1992). Despite this formal ambiguity, the angular diameter distance would have to differ quite radically from their form in GR to prevent the low number of quasar lenses observed being a serious problem for MOND.

6 CLUSTER LENSING

The central regions of galaxy clusters are very effective gravitational lenses, as evidenced by giant arcs, the strongly distorted images of background galaxies (e.g. Kneib et al. 1996). Combined with the more numerous weakly sheared images of background sources, the projected mass distributions of lensing clusters have been convincingly reconstructed in a number of cases (e.g. Mellier et al. 1993; Hammer et al. 1997; AbdelSalam et al. 1998). The inferred mass maps are generally correlated with the distribution of galaxies within the clusters, but there is also strong evidence for dark matter.

In MOND, on the other hand, the lensing signal must be solely due to the cluster members (and any gas present). Just as lensing by isolated galaxies offers a powerful test of MOND (Section 5.1), so does cluster lensing. The correlation between the mass maps and the cluster galaxies is certainly consistent with expectations, but the presence of a large number of deflectors makes a more quantitative analysis problematic. Most fundamentally, the net effect of multiple lenses is not known with any certainty, despite being well-defined in the particular formalism described in Section 2. Further, even if the lens theory was known, the lack of a thin-lens approximation results in a mass of degeneracies, with the line-of-sight location of each cluster galaxy being a free parameter. In some cases the discrepancy between theory and observation might be so severe that this ambiguity is unimportant (e.g. Beckenstein & Sanders 1994), but for the moment no strong conclusions regarding MOND can be drawn from cluster lensing.

7 CONCLUSIONS

MOND is a modification of inertia (or gravity) which can explain a variety of astronomical observations that would otherwise imply the existence of large amounts of dark matter. Lacking a relativistic analogue, however, MOND makes no definite predictions about cosmology or photon propagation. Sanders (1998) took an empirical approach to the former problem with some success, and, in a similar spirit, Mortlock & Turner (2001) showed that the existing galaxy-galaxy lensing data are consistent with the simple MONDian theory of gravitational lensing described by Qin et al. (1995).

This formalism was extended in Section 2, and can be applied to isolated mass distributions with some confidence, but, due to the counter-intuitive nature of MOND, cannot be extrapolated to multiple deflectors with any certainty. A further complication is the failure of the thin-lens approximation, which means that any ambiguities in the (three-dimensional) luminosity density of a deflector flow through to its lensing properties. These difficulties notwithstanding, this tentative theory of MONDian gravitational lensing is subject to a number of observational tests.

MOND is consistent with observations of galaxy-galaxy lensing, although tests for deviation from azimuthal symmetry in the shear signal should be able to discriminate unambiguously between dark matter and most alternative gravity theories (Section 3; Mortlock & Turner 2001). Low-optical depth microlensing within the local group is unlikely to be a particularly useful in this context, but on cosmological scales will be a very clean probe of MOND, if sufficiently many lensing events are detected (Section 4). If MOND is consistent with such simple lensing observations, more complex scenarios, such as strong lensing by galaxies and clusters, should provide additional constraints (Sections 5 and 6, respectively). Finally, the frequency of strong lensing events is already at odds with MOND, as the $\Omega_{m0} \simeq 0.01$, $\Omega_{\Lambda0} \simeq 0.99$ MONDian cosmology implied by CMB observations (McGaugh 2000) should result in many more multiply-imaged sources than are observed (Section 5.2), although there is some ambiguity in the redshift-distance relationship in such a universe.

On balance the formalism described in Section 2 is a reasonable hypothesis for gravitational lensing within the framework for MOND, and must be qualitatively correct for isolated deflectors. The theory is subject to a number of tests, although most await the completion of current surveys or further theoretical development. However it is likely that any fully relativistic extension of MOND must be completely non-linear to explain all of the above manifestations of gravitational lensing.

ACKNOWLEDGMENTS

The authors acknowledge a number of interesting discussions with Anthony Challinor, Erwin de Blok, Mike Hobson, Geraint Lewis, Stacy McGaugh, Moti Milgrom, Bohdan Paczyński, Joachim Wambsganss. DJM was funded by PPARC and this work was supported in part by NSF grant AST98-02802.

REFERENCES

- AbdelSalam H. M., Saha P., Williams L. L. R., 1998, MNRAS, 294, 734
- Afonso C., et al., 1999, A&A, 344, L63
- Alcock C., et al., 2000, ApJ, 542, 281
- Beckenstein J., Sanders R. H., 1994, ApJ, 429, 480
- Begeman K. G., Broeils A. H., Sanders R. H., 1991, MNRAS, 249, 523
- Binney J. J., Tremaine S., 1987, Galactic Dynamics. Princeton University Press, Princeton
- Brainerd T. G., Blandford R. D., Smail I. S., 1996, ApJ, 466, 623
- Carroll S. M., Press W. H., Turner E. L., 1992, ARA&A, 30, 499

Chae K.-H., Turnshek D. A., Khersonsky V. K., 1998, *ApJ*, 495, 609

Chen G. H., Kochanek C. S., Hewitt J. N., 1995, *ApJ*, 447, 62

Cheongho H., Gould A., 1996, *ApJ*, 473, 230

de Bernardis P., et al., 2000, *Nature*, 404, 955

Dyson F. W., Eddington A. S., Davidson C. R., 1920, *Mem. R. Ast. Soc.*, 62, 291

Efstathiou G., Bridle S. L., Lasenby A. N., Hobson M. P., Ellis R. S., 1999, *MNRAS*, 303, L47

Ehlers J., Schneider P., 1986, *A&A*, 168, 57

Felten J. E., 1984, *ApJ*, 286, 3

Fischer P., et al., 2000, *AJ*, 120, 1198

Garnavich P. M., Loeb A., Stanek K. Z., 2000, *ApJ*, 544, L11

Gyuk G., Crotts A., 2000, *ApJ*, 535, 621

Hammer F., Gioia I. M., Shaya E. J., Teyssandier P., Le Fevre O., Luppino, G. A., 1997, *ApJ*, 491, 477

Hannay S., et al., 2001, *ApJ*, in press

Hinshaw G., Krauss L. M., 1987, *ApJ*, 320, 468

Keeton C., Kochanek C. S., Falco E. E., 1998, *ApJ*, 509, 561

Keeton C. R., Kochanek C. S., Seljak U., 1997, *ApJ*, 482, 604

Kneib J.-P., Ellis R. S., Smail I., Couch W. J., Sharples R. M., 1996, *ApJ*, 471, 643

Kochanek C. S., 1996, *ApJ*, 466, 638

Kovner I., 1987, *ApJ*, 312, 22

Langston G. I., et al., 1989, *AJ*, 97, 1283

Lehár J., Langston G. I., Silber A., Lawrence C. R., Burke B. F., 1993, *AJ*, 105, 847

Linder E. V., 1998, *ApJ*, 497, 28

Mateo M. L., 1998, *ARA&A*, 36, 435

McGaugh S. S., 1999, *ApJ*, 523, L99

McGaugh S. S., 2000, *ApJ*, 541, L33

McGaugh S. S., de Blok W. J. G., 1998, *ApJ*, 499, 66

Mellier Y., Fort B., Kneib J.-P., 1993, *ApJ*, 407, 33

Milgrom M., 1983a, *ApJ*, 270, 365

Milgrom M., 1983b, *ApJ*, 270, 371

Milgrom M., 1983c, *ApJ*, 270, 384

Milgrom M., 1997, *ApJ*, 478, 7

Milgrom M., 1998, *ApJ*, 496, L89

Mortlock D. J., Turner E. L., 2001, *MNRAS*, submitted

Mortlock D. J., Webster R. L., 2000, *MNRAS*, 319, 860

Natarajan P., Refregier A., 2000, *ApJ*, 538, L113

Navarro J. F., Frenk C. S., White S. D. M., 1995, *MNRAS*, 275, 720

Navarro J. F., Frenk C. S., White S. D. M., 1996, *ApJ*, 462, 563

Paczynski B., 1986, *ApJ*, 304, 1

Paczynski B., 1996, *ARA&A*, 34, 419

Qin B., Wu X. P., Zou Z. L., 1995, *A&A*, 296, 264

Ratnatunga K. U., Ostrander E. J., Griffiths R. E., Im M., 1995, *ApJ*, 453, L5

Robertson D. S., Carter W. E., 1984, *Nature*, 310, 572

Sagar R., Mohan V., Pandey S. B., Pandey A. K., Stalin C. S., Castro-Tirado A. J., 2000, *Bull. Ast. Soc. India*, 28, 499

Sanders R. H., 1994, *A&A*, 284, L31

Sanders R. H., 1997, *ApJ*, 480, 492

Sanders R. H., 1998, *MNRAS*, 296, 1009

Sanders R. H., 2000, *MNRAS*, 313, 767

Schneider P., Ehlers J., Falco E. E., 1992, *Gravitational Lenses*, Springer-Verlag, Berlin

Scott D., White M., Cohn J. D., Pierpaoli E., *MNRAS*, submitted

Tadros H., Warren S. J., Hewett P. C., 2001, in Kneib J.-P., Mellier Y., Moniez M., Tran Thanh Van J., eds., *Cosmological Physics with Gravitational Lensing*. Edition Frontiers, in press

Turner E. L., 1990, *ApJ*, 365, L43

Tytler D., O'Meara J. M., Suzuki N., Lubin D., 2000 *Phys. Scr.*, 85, 12

Walker M. A., 1994, *ApJ*, 430, 463

Walker M. A., 1999, *MNRAS*, 306, 504

Walsh D., Carswell R. F., Weymann R. J., 1979, *Nature*, 279, 381

York D. G., et al., 2000, *AJ*, 120, 1579

This paper has been produced using the Royal Astronomical Society/Blackwell Science L^AT_EX style file.